**Original Research**

# In Vivo MR Imaging of Bone Marrow Cells Trafficking to Atherosclerotic Plaques

Bensheng Qiu, PhD,[1,4] Fabao Gao, MD, PhD,[1] Piotr Walczak, MD,[1,2] Jiangyang Zhang, PhD,[1] Sourav Kar, MS,[1,3] Jeff W.M. Bulte, PhD,[1,2] and Xiaoming Yang, MD, PhD[1,4]*

**Purpose:** To develop a magnetic resonance imaging (MRI)-based method to monitor in vivo trafficking of bone marrow (BM) cells to atherosclerotic lesions.

**Materials and Methods:** BM cells from LacZ-transgenic mice were labeled with a superparamagnetic iron oxide (Feridex) and then transplanted into ApoE$^{-/-}$ recipient mice that were fed an atherogenic diet. Twenty-four ApoE$^{-/-}$ mice were divided into three study groups: 1) group I with Feridex-labeled BM transplantation (BMT) cells ($N$ = 9), 2) group II with unlabeled BMT cells ($N$ = 10), and 3) group III with no BMT cells ($N$ = 5). Migrated Feridex/LacZ-BM cells to atherosclerotic aortic walls were monitored in vivo using a 4.7T MR scanner and correlated with histopathological findings.

**Results:** In group I with Feridex-BMT cells, histology examination displayed plaques in five of nine animals. In four of these five animals, in vivo MRI showed large MR signal voids of the aorta walls (due to the "blooming" effect of migrated Feridex-BM cells in plaques), which were correlated with Feridex- and/or LacZ-positive cells detected in the atherosclerotic lesions. No signal voids could be visualized in the two control animal groups (groups II and III).

**Conclusion:** This study demonstrates the potential use of in vivo MRI to monitor the trafficking of magnetically labeled BM cells to atherosclerotic lesions.

**Key Words:** atherosclerotic cardiovascular disease; bone marrow cells; magnetic resonance imaging; superparamagnetic iron oxide; magnetic cell labeling

**J. Magn. Reson. Imaging 2007;26:339–343.**


ATHEROSCLEROTIC CARDIOVASCULAR DISEASE is a unique illness that produces diffuse and multiple atherosclerotic lesions in nearly all arteries of the body. Different imaging techniques, such as digital subtraction angiography (DSA), computerized tomography (CT), ultrasound imaging, and magnetic resonance imaging (MRI), have been used to localize and characterize atherosclerotic lesions. However, none of these imaging modalities are considered an ideal imaging tool for detecting atherosclerotic lesions in the early stages. Endovascular interventional procedures, such as angioplasty with either balloon dilation or stent deployment, have been routinely used for the treatment of atherosclerotic arteries. These interventional techniques, however, function primarily as local therapies and thus do not enable the simultaneous treatment of diffuse and multiple atherosclerotic lesions around the entire body.

Previous studies have shown that hematopoietic bone marrow (BM) cells participate in the formation of different types of plaques, such as hyperlipidemia-induced atherosclerosis and transplant-associated vasculopathy (1–3). BM cells circulate in the blood system and flow through the entire body, and thus home to wherever atherosclerotic lesions exist. This characteristic of BM cells circulating throughout the body makes it possible to explore a BM-cell-mediated, plaque-specific targeting technique. Recent efforts to use MRI to serially track and quantify cell transplantation have focused on labeling the cells with MRI-detectable contrast agents, such as superparamagnetic iron-oxide agents (4–12). Once they are magnetically labeled, BM cells can carry MR contrast agents specifically to the atherosclerotic lesions, which motivated us to develop a BM-cell-mediated, plaque-specific MRI technique to guide the treatment of atherosclerotic cardiovascular disease. As a first step, in this study we validated the

[1]Russell H. Morgan Department of Radiology and Radiological Science, Johns Hopkins University School of Medicine, Baltimore, Maryland, USA.

[2]Institute for Cell Engineering, Johns Hopkins University School of Medicine, Baltimore, Maryland, USA.

[3]Department of Biomedical Engineering, Johns Hopkins University School of Medicine, Baltimore, Maryland, USA.

[4]Image-Guided Bio-Molecular Interventions, Department of Radiology, University of Washington, Seattle, Washington, USA.

Contract grant sponsor: National Institutes of Health; Contract grant numbers: HL078672; NS045062.

Bensheng Qiu and Fabao Gao contributed equally to this study.

*Address reprint requests to: X.Y., Image-Guided Bio-Molecular Interventions, Department of Radiology, University of Washington School of Medicine, 1959 NE Pacific Street, HSC AA-036, Seattle, WA 98195. E-mail: xmyang@u.washington.edu

Received April 19, 2006; Accepted February 22, 2007.

DOI 10.1002/jmri.21016

Published online in Wiley InterScience (www.interscience.wiley.com).

potential of using a noninvasive MRI method to monitor in vivo the trafficking of magnetically labeled BM cells to atherosclerotic lesions.

## MATERIALS AND METHODS

### *Animal Study Groups*

Twenty-four ApoE$^{-/-}$ mice (8–10 weeks old, B6.129P2; Jackson Laboratories) were divided into three study groups: 1) group I with magnetically labeled BM transplantation (BMT) cells ($N$ = 9), 2) group II with unlabeled BMT cells ($N$ = 10), and 3) group III with no BMT cells ($N$ = 5). All animals were fed an atherogenic diet for approximately 9–11 weeks. The animal experiments were approved by our institutional animal care and use committee and complied with NIH guidelines (13).

### *BMT*

BM cells were extracted from 19 donor mice (i.e., transgenic mice expressing a biomarker, β-galactosidase (LacZ) (B6; 129S7-Gtrosa26, Jackson Laboratories, Bar Harbor, ME, USA)). The femurs and tibias of the donor mice were first excised. Then the marrows were flushed using a syringe with a 28-gauge needle and collected in a tube. After the red blood cells were lysed, the LacZ-BM cells were labeled in vitro with a superparamagnetic iron-oxide MR contrast agent (Feridex; Berlex Laboratories, Wayne, NJ, USA) as previously described (14,15).

In animal groups I and II, before BMT the 19 recipient ApoE$^{-/-}$ mice were irradiated with a dose of 900 rads ($N$ = 15) or 370 rads ($N$ = 4) (Gammacell 40; MDS Nordion, Ottawa, Canada). Subsequently, the labeled ($N$ = 9) and unlabeled ($N$ = 10) LacZ-BM cells were transplanted into the recipient mice by tail-vein injection. Each recipient mouse received approximately $8 \times 10^6$ cells suspended in 0.3–0.4 mL of 10 mM phosphate-buffered saline (PBS). In animal group III, five ApoE$^{-/-}$ mice that did not undergo irradiation or BMT served as controls.

Approximately four weeks after BMT, the animals were placed on an atherogenic diet (15% butter and 2% cholesterol, RD Western Diet; Research Diets, Inc., New Brunswick, NJ, USA) to induce hyperlipidemia and subsequent atherosclerotic lesions (2,16).

### *In Vivo MRI of BM Cells Trafficking to Atherosclerotic Arteries*

Approximately 13–15 weeks after BMT, in vivo visualization of migrated Feridex/LacZ-BM cells to the atherosclerotic lesions of the aortas was performed on a 4.7T MR imager (Bruker Biospin, Billerica, MA, USA)

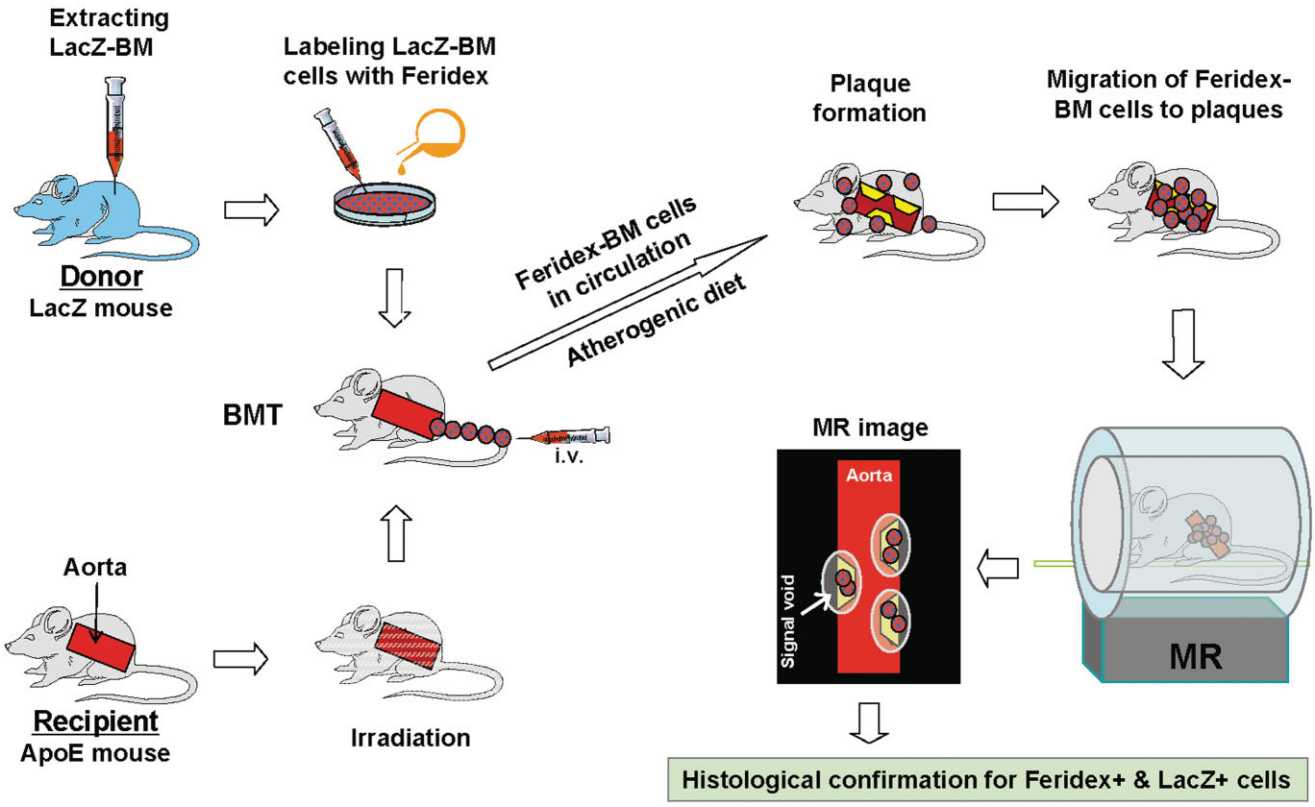


**Figure 1.** The experimental protocol. BM is extracted from a donor LacZ-expressing mouse, and BM cells are labeled in vitro with Feridex. Feridex-labeled BM cells are then transplanted intravenously into the irradiated recipient ApoE$^{-/-}$ mouse, which is then fed an atherogenic diet. Following the formation of atherosclerosis, the Feridex-labeled BMT cells migrate into the plaque sites. Subsequently, in vivo MR images are obtained that show large MR signal voids of the aortic wall. The targeted aorta is then harvested to correlate the MR images with histological staining of tissues for Feridex- or LacZ-positive cells. [Color figure can be viewed in the online issue, which is available at www.interscience.wiley.com.]

with a 35-mm birdcage coil (Bruker Biospin, Billerica, MA, USA). The mice were positioned in the supine position and a pressure-sensitive pad for respiratory gating was placed on the abdomen. Electrocardiograms (ECG) were observed by insertion of two ECG needles (SA Instruments, Inc., Stony Brook, NY, USA) to the right-upper and left-lower extremities of the animals. During imaging the mice were anesthetized with 1.0% to 1.5% isoflurane, with air and oxygen mixed at a 3:1 ratio. We regulated the flow of isoflurane to maintain the respiratory rate at approximately 100 breaths per minute and the heart rate at approximately 400 beats per minute. The ECG and respiratory signals were used to synchronize image acquisition to reduce imaging artifacts due to cardiac and respiratory motions. The in vivo imaging parameters included a fast spin-echo (FSE) sequence (repetition time (TR) = 2 seconds; echo time (TE) = 13.4 msec; echo train length (ETL) = 4; four signal averages, slice thickness = 1 mm; 12 slices with no gap; field of view (FOV) = 22 mm × 22 mm, matrix = 256 × 256, and an in-plane resolution = 0.08 × 0.08 $mm^2$). The total imaging time was approximately 15 minutes depending on the respiratory and heart rates of each animal. We chose the FSE sequence because it provides superior image quality for monitoring aortic morphology compared to a gradient-echo sequence at high field strength.

### *Histological Correlation*

The animals were anesthetized by intraperitoneal injection of 100–150 μL pentobarbital (0.25–0.38 mg/g) and then euthanized by perfusing the animal with 4% paraformaldehyde via an open-chest, left-cardiac-ventricle puncture approach. This perfusion-fixation method enabled the removal of all blood from the animal body, and endovascular fixation. The ascending aorta was selected as the primary region of interest (ROI) for MRI and histological correlation because 1) the ascending aorta is the largest vessel in a mouse, and thus enables optimal imaging; 2) the root of the ascending aorta is the primary target of atherosclerotic lesions; and 3) the cardiac base is a useful landmark for allocating the target segment of the ascending aorta for precise correlation between MRI and tissue harvesting. Thus an approximately 5-mm-long segment of the ascending aorta, measured from the cardiac base, was harvested from all mice. Subsequently the tissues were cryosectioned at 10-μm slice thickness and the slices of the aortic tissues were stained with 1) hematoxylin and eosin (H&E) for histology examination to grade the atherosclerotic lesions, and 2) Prussian blue and X-gal for histochemical staining to detect Feridex- and LacZ-positive cells at the targets. A previous study extensively evaluated the phenotypes of migrated BM cells that localize in the area of hyperlipidemia-induced atherosclerosis, and found that they primarily give rise to smooth muscle cells (SMCs) (17). Thus, in the present study we did not attempt to determine whether BM cells remain in an undifferentiated form or follow downstream differentiation pathways.

Figure 1 summarizes the overall experimental protocol for in vivo MRI to monitor trafficking of BM cells to atherosclerotic lesions.

### *Image Analysis*

Images were reconstructed using the scanner console (Paravision; Bruker Biospin, Billerica, MA, USA) and analyzed using Amira software (Mercury Computer Systems Inc., San Diego, CA, USA). For analysis of MRI, the ascending aortic wall was qualitatively scored by a grading system as follows: 1) the thoracic structures, including the aorta, were not identifiable due to poor quality of the images; 2) the aortic wall appeared as a bright ring; and 3) the aortic wall manifested as large MR signal voids (disappearance of more than one-quarter of the aortic walls). For histological correlation, atherosclerotic lesions of the aorta tissues were qualitatively scored by a grading system as 1) normal aortic wall, 2) intimal hyperplasia, and 3) plaque formation (representing both the lipid core and fibrous cap). Animals with either unidentifiable thoracic structures on MRI or normal aortic walls on histology were excluded from the final data analysis.

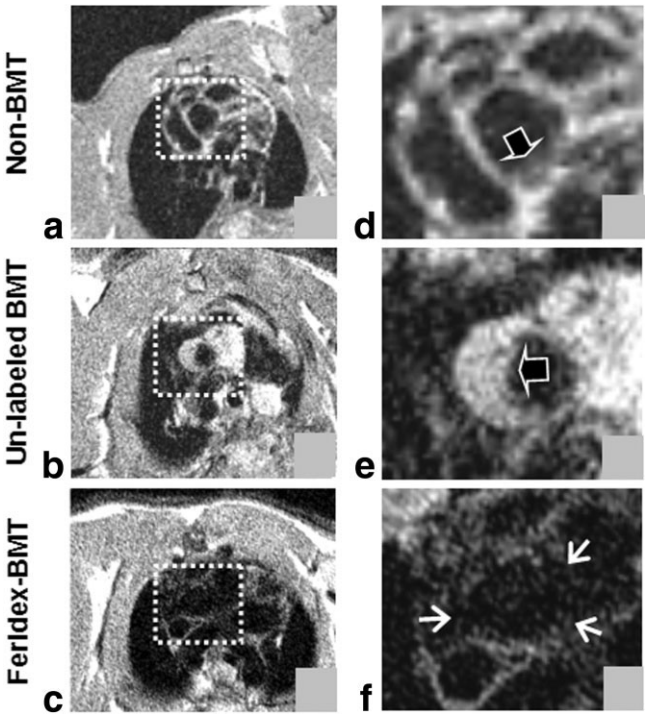


**Figure 2. a–c:** Cross-sectional view of in vivo 4.7T MR images of different aortas following the various treatments. Insets outline the ascending aorta, showing a large MR signal void of the aortic wall in animal (c) with Feridex-labeled BMT cells, while the aortas in animals a and b appear as bright rings. **d–f:** Magnification of insets of (a–c). On images (d) and (e) (treated with no BMT or unlabeled BMT), atherosclerotic plaques are visualized as thickening of the aortic walls (open arrows), and the aorta are basically shown as bright rings. On image (f) (treated with Feridex-labeled BMT), larger signal voids (arrows) of the aortic wall are seen due to the "blooming" effect of Feridex-labeled cells trafficking to the atherosclerotic aortic wall.

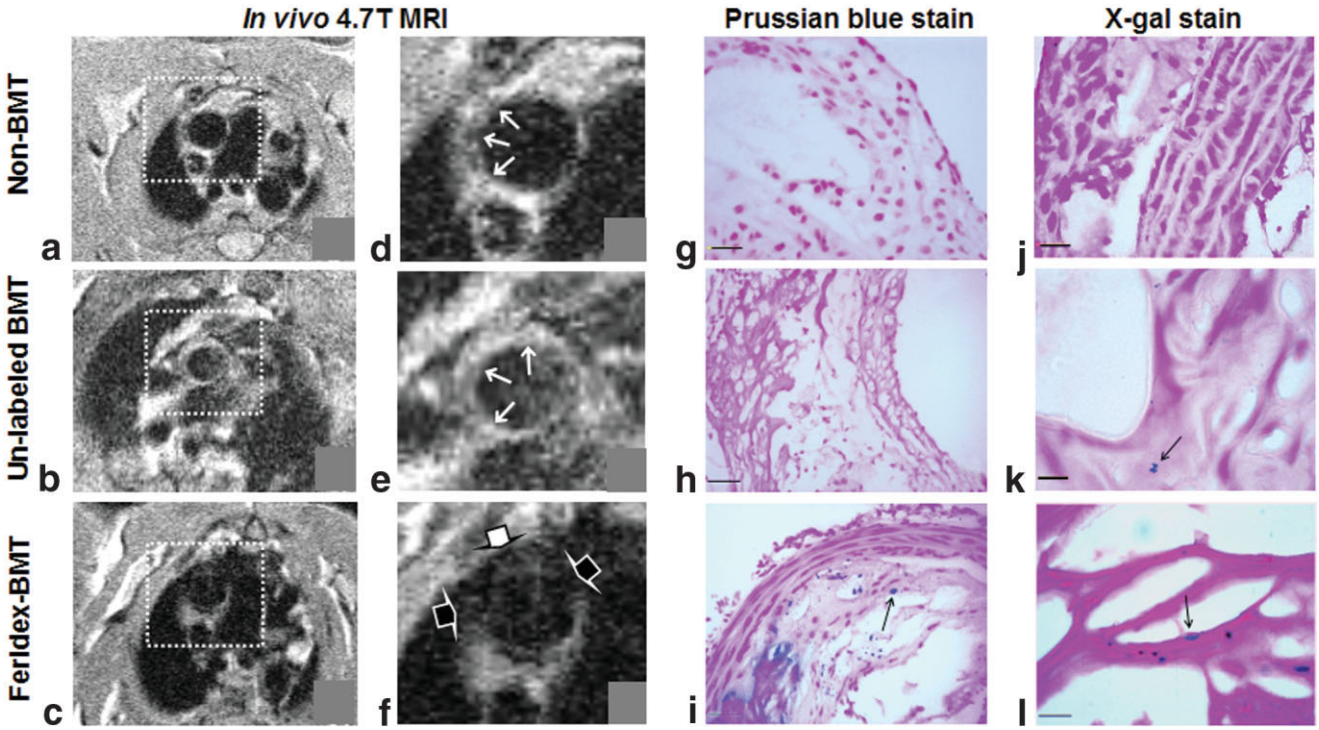


**Figure 3. a–c:** Cross-sectional view of representative in vivo 4.7T MR images of aortas from different animals. Insets outline the ascending aorta, showing a large MR signal void of the aortic wall in animal (c) with Feridex-labeled BMT cells, while the aortas of animals (a) and (b) appear as bright rings. **d–f:** Magnification of insets of (a–c). On images (d) and (e) (treated with no BMT and unlabeled BMT), the thickened aortic walls due to atherosclerotic plaques (arrows) are visualized and the aortic walls are basically shown as bright rings. On image (f) (treated with Feridex-labeled BMT), larger signal voids (open arrows) of the aortic wall are seen. **g–i:** Histochemical staining for Feridex with Prussian blue (scale bar = 50 μm). **j–l:** Histochemical staining for LacZ with X-gal (scale bar = 20 μm). Numerous Feridex- and LacZ-positive cells (blue color, arrows) are detected in aortic tissues with BMT (k, i, and l) that are not visualized in the control aortic tissues (g, j and h).

## RESULTS

BMT was performed successfully in all recipient mice. Four of 10 cases in group II showed unidentifiable thoracic structures on MRI, primarily due to unstable heart rates and respiration artifacts. Thus, these four cases were excluded from the final data analysis. In the remaining 20 cases, histological grading showed the formation of atherosclerotic plaques in 15 cases and intimal hyperplasia in five cases.

In animal group I with Feridex-BM cell transplantation, in vivo MRI revealed large MR signal voids of the aortic walls in four cases (Fig. 2). In all of these cases, histological examination diagnosed the formation of atherosclerotic plaques, and histochemistry detected Feridex- and/or LacZ-positive cells in the aortic tissues (Fig. 3).

In animal groups II and III, in vivo MRI did not detect large MR signal voids, and presented only the aorta as a bright ring in all 11 cases (Table 1). Subsequent histology examination graded atherosclerotic plaques in 10 cases and intimal hyperplasia in one case. Histochemistry detected LacZ-positive cells in four cases of animal group II with transplantation of unlabeled BM cells, while there were no Feridex-positive cells in any of the animals in groups II and III. In one case in group III, the calcification of plaque was stained blue with histochemistry.

Of the 15 animals that had histologically-confirmed atherosclerotic plaques, in vivo MRI detected plaques in 12 cases, with missed plaques in three cases. In the five animals that had histologically-confirmed intimal hyperplasia, no plaques were detected by in vivo MRI, which presented the aortas of the five animals as bright rings.

Figure 3 compares representative images of in vivo MRI and histochemistry obtained from the different an-

Table 1
Summarized Results

| Animal groups | BM transplant | In vivo MRI | | | Histology | | Histochemistry | |
|---|---|---|---|---|---|---|---|---|
| | | Normal (as ring) | Visible plaques | Signal voids | Intimal hyperplasia | Plaque | Feridex+ | LacZ+ |
| Group 1 ($N$ = 9) | Feridex-labeled | 5 | 4 | 4 | 4 | 5 | 6 | 6 |
| Group 2 ($N$ = 6) | Unlabeled | 6 | 4 | — | 1 | 5 | — | 4 |
| Group 3 ($N$ = 5) | None | 5 | 4 | — | — | 5 | — | — |

imal groups with various treatments. Table 1 summarizes the results of the three animal groups.

## DISCUSSION

Previous cardiac MRI studies using large animal models demonstrated the successful visualization of locally injected Feridex-labeled stem cells in the myocardium (14,18). Using in vivo MRI to detect magnetically labeled BM cells in the mouse aorta is a much more challenging task. To the best of our knowledge, the current study represents the first attempt to validate the possibility of using noninvasive MRI to monitor trafficking of BM cells to the site of hyperlipidemia-induced atherosclerosis.

The initial results of this study indicate that BM-derived cells contribute to the formation of plaques, manifested as a localization of Feridex- and/or LacZ-positive cells at the atherosclerotic aortic walls, and thus it is possible to visualize Feridex-labeled LacZ-BM cells that have migrated to atherosclerotic lesions using in vivo MRI. The MRI hallmark of migrated Feridex/LacZ-BM cells to plaque areas is the pronounced large MR signal void of the aortic wall (caused by the "blooming" of Feridex), which was not visualized in the two control animal groups with either unlabeled BMT cells transplantation or no BMT cells.

This study also shows that in all five aortas with intimal hyperplasia only (rather than plaque formation), there were no large MR signal voids of the aortic walls under in vivo MRI. This result may indicate that the ability to use in vivo MRI to detect Feridex-labeled cells in the vessel walls increases as Feridex/LacZ-BM cell-involved atherosclerotic lesions enlarge.

To achieve high-quality MR images, it is critical for the mice to be in a stable physiological condition. In 24 atherosclerotic mice, we were not able to identify the thoracic structures in four cases and missed atherosclerotic plaques in three cases under in vivo MRI. The potential reasons for this include unstable heart rates of the mice leading to unsatisfactory ECG gating, and artifacts caused by irregular respiratory patterns. These factors, in their severe form, can reduce the signal-to-noise ratio (SNR) and make it difficult to image these very small plaques within the thin mouse aortic walls using a 4.7T MR scanner. This study did not allow us to determine the minimum amounts of Feridex-positive cells within the atherosclerotic lesion that can generate discernible MR signals. This likely explains why only four of the six animals with Feridex/LacZ-positive cells showed large signal voids of the aortas on MRI (see Table 1). In addition, previous studies from other groups reported that intravenous injection of Feridex led to labeling of microphages in a number of lesions, including atherosclerotic plaques (19,20). Thus, it is warranted to further investigate the possibility that death of the labeled cells releases Feridex particles, which may then be taken up by macrophages.

An MRI-based in vivo cell-tracking technique should facilitate further noninvasive investigations of the role of specific hematopoietic BM cells in the pathogenesis of hyperlipidemia-induced atherosclerosis and transplant-associated arteriosclerosis. It may also provide a useful method to guide the targeting of BM cells for gene therapy or chemotherapy of atherosclerosis when loading genes or drugs into the plaque-specific BM cells.

In conclusion, this study demonstrates the potential use of MRI to monitor in vivo the trafficking of magnetically labeled BM cells to atherosclerotic lesions.

## ACKNOWLEDGMENT

The authors thank Ms. Mary McAllister for her editorial assistance.

## REFERENCES

1. Krause D, Theise N, Collector M, et al. Multi-organ, multi-lineage engraftment by a single bone marrow-derived stem cell. Cell 2001; 105:369–377.
2. Sata M, Saiura A, Kunisato A, et al. Hematopoietic stem cells differentiate into vascular cells that participate in the pathogenesis of atherosclerosis. Nat Med 2002;8:403–409.
3. Werner N, Junk S, Laufs U, et al. Intravenous transfusion of endothelial progenitor cells reduces neointima formation after vascular injury. Circ Res 2003;93:e17–24.
4. Shapiro E, Sharer K, Skrtic S, Koretsky A. In vivo detection of single cells by MRI. Magn Reson Med 2006;55:242–249.
5. Heyn C, Ronald J, Mackenzie L, et al. In vivo magnetic resonance imaging of single cells in mouse brain with optical validation. Magn Reson Med 2006;55:23–29.
6. Schoepf U, Marecos E, Melder R, Jain R, Weissleder R. Intracellular magnetic labeling of lymphocytes for in vivo trafficking studies. Biotechniques 1998;24:642–646.
7. Kircher M, Allport J, Graves E, et al. In vivo high resolution three-dimensional imaging of antigen-specific cytotoxic T-lymphocyte trafficking to tumors. Cancer Res 2003; 63:6838–6846.
8. Anderson S, Shukaliak-Quandt J, Jordan E, et al. Magnetic resonance imaging of labeled T-cells in a mouse model of multiple sclerosis. Ann Neurol 2004;55:654–659.
9. de-Vries I, Lesterhuis W, Barentsz J, et al. Magnetic resonance tracking of dendritic cells in melanoma patients for monitoring of cellular therapy. Nat Biotechnol 2005;23:1407–1413.
10. Bos C, Delmas Y, Desmouliere A, et al. In vivo MR imaging of intravascularly injected magnetically labeled mesenchymal stem cells in rat kidney and liver. Radiology 2004;233:781–789.
11. Hauger O, Frost E, van-Heeswijk R, et al. MR evaluation of the glomerular homing of magnetically labeled mesenchymal stem cells in a rat model of nephropathy. Radiology 2006;238:200–210.
12. Daldrup-Link H, Rudelius M, Oostendorp R, et al. Comparison of iron oxide labeling properties of hematopoietic progenitor cells from umbilical cord blood and from peripheral blood for subsequent in vivo tracking in a xenotransplant mouse model. Acad Radiol 2005; 12:502–510.
13. National Institutes of Health. Guide for the care and use of laboratory animals. NIH publication no. 86-23, Bethesda: NIH; 1985.
14. Kraitchman D, Heldman A, Atalar E, et al. In vivo magnetic resonance imaging of mesenchymal stem cells in myocardial infarction. Circulation 2003;107:2290–2293.
15. Frank J, Miller B, Arbab A, et al. Clinically applicable labeling of mammalian and stem cells by combining superparamagnetic iron oxides and transfection agents. Radiology 2003;228:480–487.
16. Johnson J, Carson K, Williams H, et al. Plaque rupture after short periods of fat feeding in the apolipoprotein E-knockout mouse: model characterization and effects of pravastatin treatment. Circulation 2005;111:1422–1430.
17. Xu Y, Arai H, Zhuge X, et al. Role of bone marrow-derived progenitor cells in cuff-induced vascular injury in mice. Arterioscler Thromb Vasc Biol 2004;24:477–482.
18. Hill J, Dick A, Raman V, et al. Serial cardiac magnetic resonance imaging of injected mesenchymal stem cells. Circulation 2003;108: 1009–1014.
19. Schmitz S, Coupland S, Gust R, et al. Superparamagnetic iron oxide-enhanced MRI of atherosclerotic plaques in Watanabe hereditable hyperlipidemic rabbits. Invest Radiol 2000;35:460–471.
20. Rogers W, Basu P. Factors regulating macrophage endocytosis of nanoparticles: implications for targeted magnetic resonance plaque imaging. Atherosclerosis 2005;178:67–73.